Published in final edited form as:
Mol Cancer Ther. 2010 December ; 9(12): . doi:10.1158/1535-7163.MCT-10-0305.

Nakiterpiosin Targets Tubulin and Triggers Mitotic Catastrophe in Human Cancer Cells

Jen-Hsuan Wei and **Joachim Seemann**
Department of Cell Biology, University of Texas Southwestern Medical Center, Dallas, TX 75390, USA

Abstract

Agents that interfere with mitotic progression by perturbing microtubule dynamics are commonly used for cancer chemotherapy. Here, we identify nakiterpiosin as a novel anti-mitotic drug that targets microtubules. Nakiterpiosin induces mitotic arrest and triggers mitotic catastrophe in human cancer cells by impairing bipolar spindle assembly. At higher concentration, it alters the interphase microtubule network and suppresses microtubule dynamics. In the presence of nakiterpiosin, microtubules are no longer arranged in a centrosomal array and centrosome-mediated microtubule regrowth after cold depolymerization is inhibited. However, centrosome organization, the ultrastructure of Golgi stacks and protein secretion are not affected, suggesting that the drug has minimal toxicity towards other cellular functions. Nakiterpiosin interacts directly with tubulin, inhibits microtubule polymerization *in vitro*, and decreases polymer mass in cells. Furthermore, it enhances tubulin acetylation and reduces viability of paclitaxel-resistant cancer cells. In conclusion, nakiterpiosin exerts anti-proliferative activity by perturbing microtubule dynamics during mitosis, which activates the spindle assembly checkpoint and triggers cell death. These findings suggest the potential use of nakiterpiosin as a chemotherapeutic agent.

Keywords

nakiterpiosin; microtubule; anti-mitotic; cancer; paclitaxel resistance

Introduction

Cancer chemotherapy relies primarily on agents called anti-mitotics which prevent or interfere with mitotic progression (1). These compounds have proven widely successful and currently all such drugs in clinical use target microtubules. Microtubules are dynamic cytoskeletal filaments essential for a wide variety of cellular processes such as chromosome segregation (2), organelle positioning (3), protein trafficking (4) and ciliogenesis (5). Composed of α- and β-tubulin heterodimers, microtubules alternate between phases of growth and shrinkage, a process termed dynamic instability (6). In interphase, microtubules are normally arranged into a radial array emanating from the centrosomes (7). Upon entry into mitosis, the microtubule network is disassembled to allow assembly of the mitotic spindle. At this transition, the dynamic instability of microtubules is significantly increased (8), making it an excellent target for microtubule poisons to interfere with mitosis. In contrast to most cells in the human body that are post-mitotic, cancer cells have the ability to proliferate and divide autonomously. By perturbing microtubule dynamics during cell

Correspondence to: Joachim Seemann, Department of Cell Biology, University of Texas Southwestern Medical Center, 5323 Harry Hines Blvd, Dallas, TX 75390, USA; Tel: 214-648-0317; Fax: 214-648-9093; joachim.seemann@utsouthwestern.edu.

division, which in turn induces mitotic arrest and cell death, highly proliferative cancer cells can be selectively eliminated.

Nakiterpiosin was initially isolated from a marine sponge as a potent cytotoxic compound against mouse leukemia P388 cells (9). Furthermore, it was recently shown that a synthetic form (for structure, see Fig. 1) caused loss of the primary cilium and thus reduced Hedgehog (Hh) signaling in NIH3T3 mouse fibroblasts (10). Therefore, nakiterpiosin has been suggested to function as an Hh antagonist that could be used against Hh-dependent tumors.

In this paper, we identify nakiterpiosin as a novel microtubule-targeting agent that triggers mitotic catastrophe in cancer cells. Surprisingly, we found that nakiterpiosin alters microtubule dynamics, which is an entirely different mechanism of action than previously reported (10). Nakiterpiosin induces mitotic arrest and cell death by impairing spindle assembly. In addition to mitotic abnormalities, nakiterpiosin also causes interphase defects including disintegration of the centrosomal microtubule array and suppression of microtubule dynamics. However, protein secretion is not affected. Nakiterpiosin interacts directly with tubulin, inhibits microtubule polymerization, enhances tubulin acetylation, and reduces the viability of paclitaxel-resistant cancer cells. In summary, we report the first identification of nakiterpiosin as a novel anti-mitotic agent and a detailed characterization of its effects on microtubules. These findings highlight the potential of nakiterpiosin as a chemotherapeutic agent.

Materials and Methods

Cell culture, antibodies and reagents

HeLa cells were obtained from the American Type Culture Collection and were grown in DMEM containing antibiotics (Mediatech) and 10% cosmic calf serum (CCS) (HyClone). Cells from early-passage (<10) stocks were used without further authentication. NCI-H1155 and HCC366 cells were obtained in June 2010 from the laboratory of Michael A. White and were DNA fingerprinted and confirmed in March 2010 in the laboratory of John D. Minna (University of Texas Southwestern Medical Center, Dallas, TX). The cells were used within two months of receipt and were grown in RPMI 1640 (Invitrogen) containing antibiotics and 5% CCS as previously described (11). The following primary antibodies were used: mouse monoclonal antibodies against α-tubulin (TAT1, K. Gull), acetylated α-tubulin (6-11B-1, Sigma), γ-tubulin (GTU-88, Sigma), BubR1 (Upstate Biotechnology), CD8 (OKT8, F. Watt), rabbit polyclonal antibodies against α-tubulin (Thermo Fisher Scientific), EB1 (Sigma), pericentrin (Covance and Abcam), γ-tubulin (Axyll), GM130 (MLO7, M. Lowe), and human CREST autoimmune serum (ImmunoVision). The following secondary antibodies were used: anti-mouse and anti-rabbit conjugated to AlexaFluor 488, 555, 594 or 647 (Invitrogen), Cy2-conjugated anti-human, and HRP-conjugated anti-mouse and anti-rabbit antibodies (Pierce). Hoechst 33342 was from Invitrogen. Nocodazole and paclitaxel were from Sigma. Synthetic nakiterpiosin was provided by Chuo Chen (10). All drugs were dissolved in DMSO.

In vitro tubulin polymerization assay

The fluorescence-based *in vitro* tubulin polymerization assay was performed according to the manufacturer's instructions (Cytoskeleton) at 37°C with 2 mg/ml bovine brain tubulin (> 99% pure), 1 mM GTP and the indicated drugs. Reactions were monitored by emission at 450 nm.

Determination of microtubule polymer mass

HeLa cells treated with vehicle or drugs for 2 h were lysed at room temperature with 80 mM PIPES pH 6.8, 1 mM $MgCl_2$, 1 mM EGTA, 0.5% NP40, and 2 μM paclitaxel. Supernatant and pellet fractions were separated by centrifugation at 13,000 rpm for 5 min at room temperature. Equal volumes were immunoblotted for α-tubulin. The "Gels" function of ImageJ was employed to quantify band intensity.

Microtubule regrowth assay

HeLa cells were placed on ice for 30 min to depolymerize microtubules, then incubated on ice for another 30 min with vehicle or 25 μM nakiterpiosin, warmed to 37°C to initiate microtubule regrowth and fixed with methanol at the indicated time points.

Immunofluorescence

Immunostaining was performed as described (12). Images were acquired using LD Plan-Neofluar 40x/1.3 DIC and Plan-Apochromat 63x/1.4 DIC objectives, an Axiovert 200M microscope (Zeiss), an Orca 285 camera (Hamamatsu) and the software Openlab 4.0.2 (Improvision). To determine the spindle length, the "Measure" function of ImageJ was employed and the shortest distance between two γ-tubulin foci was averaged. The statistical significance was determined by unpaired, two-tailed student's t test.

Live cell imaging

Vehicle- and drug-treated cells were imaged in parallel using a motorized stage (Märzhäuser) in CO_2-independent medium containing 2 mM GlutaMAX (Invitrogen) and 10% CCS. Images were taken every 5 min with an A-PLAN 20x/0.3 Ph1 objective, an Axiovert 200M microscope (Zeiss), a Retiga 2000R camera (QImaging) and the software MetaMorph 7.1.3 (Molecular Devices).

Microinjection and CD8 transport assay

0.2 mg/ml pcDNA-CD8 and 2.5 mg/ml of lysine-fixable Texas Red-dextran (Invitrogen) were co-injected into the nuclei as described (13). 100 μg/ml cycloheximide was included during the microinjection period to prevent protein synthesis. Cycloheximide was then washed out to allow expression and transport of CD8 and the cells were then incubated with the indicated drugs. After 90 min at 37°C, cells were fixed in 3.7% formaldehyde without permeabilization and stained for CD8.

Electron microscopy

EM analysis of cells grown on glass coverslips was performed as described (14). For negative staining of microtubules, the end products of the polymerization reactions were fixed by diluting with equal volume of 2.5% glutaraldehyde in 100 mM sodium cacodylate, pH 7.4 (pre-warmed to 37°C). Samples were absorbed on glow-discharged formvar-coated grids, stained with 2% uranyl acetate and washed with water (15). Images were captured using a USC1000 2k CCD camera (Gatan) and a Tecnai G2 Spirit EM (FEI).

Cell viability assay

HeLa, NCI-H1155 and HCC366 cells were grown for 48 h in the presence of vehicle or the indicated drugs. Cell viability was then determined by the relative amount of ATP present (normalized to vehicle-treated cells) using the CellTiter-Glo luminescent cell viability assay according to the manufacture's instructions (Promega).

Results

Nakiterpiosin arrests cells in mitosis and causes mitotic catastrophe

To determine the effects of nakiterpiosin, we monitored human cervical carcinoma HeLa cells treated with varying concentrations of nakiterpiosin for 24 h using phase-contrast time-lapse microscopy. The majority of cells treated with 1 μM or less nakiterpiosin entered mitosis and progressed through cytokinesis (data not shown). In contrast, cells treated with 5 μM or more also entered mitosis but became arrested, as indicated by a gradual accumulation of rounded-up mitotic cells (Fig. 2A, from -24:00 to 0:00). The mitotic arrest was not due to long-term imaging, as control cells treated with vehicle and imaged in parallel divided normally (Supplementary Fig. S1). In addition, we observed extensive membrane blebbing in some nakiterpiosin-treated cells that died after prolonged mitotic arrest (Fig. 2A, arrows; Supplementary Fig. S1). This suggests that nakiterpiosin kills cells by inducing mitotic catastrophe, a form of cell death that occurs during mitosis (16).

We then investigated whether the mitotic block is reversible. After imaging the cells for 24 h in nakiterpiosin, we removed the drug and imaged the cells for an additional 24 h (Fig. 2A, from 0:00 to +24:00). Upon nakiterpiosin washout, the arrested cells divided and appeared healthy for the duration of the experiment (Fig. 2A, arrowheads). The reversibility implies that nakiterpiosin interferes with mitotic progression through non-covalent binding to its cellular target and does not involve any chemical modification.

Nakiterpiosin impairs spindle assembly and chromosome alignment

The live cell imaging data showed that nakiterpiosin-treated cells entered mitosis but were blocked from exiting, indicating that the spindle assembly checkpoint (SAC) could not be satisfied. To verify that nakiterpiosin induces SAC activation, we examined whether SAC proteins are recruited to the kinetochores. HeLa cells treated for 2 h with vehicle or 5 μM nakiterpiosin were stained for DNA, the SAC kinase BubR1 and with CREST serum to mark kinetochores. In vehicle-treated cells, BubR1 was localized to kinetochores after mitotic entry (Fig. 2B, prophase) but was displaced upon chromosome segregation (Fig. 2B, anaphase). Kinetochore targeting of BubR1 was clearly detected in nakiterpiosin-arrested cells, indicating that the SAC was indeed activated (Fig. 2B, NAK). To further confirm that the mitotic arrest is caused by defects in spindle assembly, we analyzed spindle morphology of drug-treated cells. HeLa cells were co-stained for α-tubulin to visualize microtubules, γ-tubulin to detect the spindle poles, and DNA to label chromosomes. Nearly all vehicle-treated cells in metaphase displayed normal bipolar spindles with condensed chromosomes properly aligned at the metaphase plate (Fig. 2C, normal). In contrast, nakiterpiosin-arrested cells exhibited a range of spindle abnormalities, which can be categorized into three major types (170 mitotic cells counted; Fig. 2C, NAK). 57% of mitotic cells assembled bipolar-like spindles but chromosome alignment was not as compact as in control cells (Fig. 2C, type I). In most cases, uncongressed chromosomes were found in close proximity to the spindle poles (Fig. 2C, arrowheads). 34% of mitotic cells formed multiple asters with chromosomes appearing as an irregular-shaped DNA mass (Fig. 2C, type II). The remaining 9% of mitotic cells developed monopolar spindles where chromosomes were arranged in a circular configuration (Fig. 2C, type III).

When we increased the concentration to 10 μM, we observed a lower percentage of bipolar-like spindles. Instead, multiple asters became the dominant phenotype. Interestingly, these asters tended to cluster together rather than spread throughout the cytoplasm (data not shown). At 25 μM, the spindles severely degenerated into small asters or punctate aggregates and, in some cases, were entirely depolymerized (data not shown). At this concentration, the chromosomes appeared less condensed.

The spindle length is decreased by nakiterpiosin

While analyzing spindle abnormalities induced by 5 μM nakiterpiosin, we noticed that bipolar-like spindles were much smaller. To evaluate the difference, we measured the spindle length in vehicle-and drug-treated cells, as determined by the distance between two γ-tubulin foci at metaphase spindle poles. Upon treatment with 5 μM nakiterpiosin, the interpolar distance was dramatically decreased by 42%, from 11.5 ± 0.2 μm in control cells to 6.7 ± 0.1 μm in drug-treated cells (25-27 spindles per condition; $P < 0.0001$; Fig. 2D). These data, together with other observed spindle defects, suggest that nakiterpiosin blocks cells in mitosis by interfering with spindle assembly.

Nakiterpiosin alters interphase microtubule organization

Because of the inhibitory effect on spindle assembly, we investigated whether nakiterpiosin alters the interphase microtubule network. HeLa cells were treated for 2 h with 5 μM nakiterpiosin or, as controls, incubated with vehicle, 5 μg/ml nocodazole, 1 μM paclitaxel or cooled on ice for 30 min (Fig. 3A). In vehicle-treated cells, microtubules concentrated in the perinuclear region and extended outwards to the cell periphery (Fig. 3A, DMSO). As expected, filaments were completely depolymerized upon nocodazole or cold treatment, as indicated by the hazy fluorescence staining of α-tubulin throughout the cytoplasm (Fig. 3A, NOC and cold). In contrast, stabilization of microtubules by paclitaxel induced parallel bundles (Fig. 3A, PTX). Interestingly, although low concentration of nakiterpiosin caused prominent mitotic arrest and aberrant mitotic phenotypes (Fig. 2), the interphase microtubule network seemed virtually unaffected and resembled the characteristic centrosomal array in control cells (Fig. 3A, NAK 5 μM).

Since microtubules exhibit less dynamic instability in interphase than in mitosis (17), we reasoned that interphase microtubules might be less sensitive to nakiterpiosin. To address this, we increased the concentration and examined the organization of the interphase network. When treated with 25μM nakiterpiosin, microtubules became extremely distorted, and most strikingly, no longer originated from the centrosomes or fully extended to the cell periphery (Fig. 3A, NAK 25 μM, the cell border is outlined with dash lines). Instead, they appeared shorter and twisted together. Moreover, the cell periphery was often devoid of filaments, suggesting that microtubules were shortened and might not reach the cell cortex due to partial depolymerization.

Nakiterpiosin displaces EB1 from microtubule tips

EB1 is a microtubule-associated protein that preferentially binds to the plus end of growing microtubules and is often used as a marker for microtubule dynamics (18). In addition to the role in regulating microtubule dynamics, EB1 also facilitates the capture and stabilization of microtubule tips at the cell cortex (18). Since microtubules frequently lose their contact with the cell periphery when treated with high concentration of nakiterpiosin (Fig. 3A, NAK 25 μM), we examined whether the drug alters EB1 localization. In vehicle-treated cells, EB1 was concentrated at the microtubule tips (Fig. 3B, DMSO), but became cytosolic upon nocodazole or cold treatment (Fig. 3B, NOC and cold). In cells treated with 5 μM nakiterpiosin, EB1 remained accumulated at the tips of microtubules, although the intensity and the length of the labeling were slightly diminished (Fig. 3B, NAK 5 μM). This is in contrast to paclitaxel-treated cells where EB1 decorated the entire length of filaments with relatively low affinity (Fig. 3B, PTX). Likewise, in cells exposed to 25μM nakiterpiosin, EB1 no longer concentrated at the tips and only weakly associated with the remaining filaments (Fig. 3B, NAK 25 μM). This suggests that high concentration of nakiterpiosin suppresses microtubule dynamics in interphase.

Nakiterpiosin inhibits microtubule growth from the centrosomes

Since 25 μM nakiterpiosin alters microtubule organization, we determined whether it affects the growth of new filaments. HeLa cells were placed on ice for 30 min to depolymerize microtubules and incubated on ice for another 30 min with vehicle or 25 μM nakiterpiosin. Subsequently cells were warmed to 37°C to initiate microtubule regrowth, fixed at various time points and stained for α-tubulin to visualize microtubules (Fig. 3C) and for pericentrin to label centrosomes (Fig. 3C, insets). At time point zero, both vehicle- and nakiterpiosin-treated cells displayed diffuse, cytoplasmic staining for α -tubulin due to complete depolymerization of microtubules (Fig. 3C, DMSO and NAK 25 μM, 0 min). Upon initiation of regrowth, centrosomal microtubule asters appeared in control cells within 1.5 min. After 5 min, more microtubules grew from the centrosomes and many filaments were also detected in the cytoplasm. After 15 min, microtubules were reorganized into a characteristic radial array emanating from the centrosomes and extending towards the cell periphery (Fig. 3C, DMSO). In contrast, centrosome-mediated microtubule regrowth was severely impaired by high concentration of nakiterpiosin. Although a faint signal for α-tubulin was detectable at the centrosomes, microtubules failed to elongate from these foci during the assay (up to 2 h) (Fig. 3C, NAK 25 μM). In contrast, numerous microtubules nucleated throughout the cytoplasm within 1.5 min. After 5 min until the end point of the assay, the cytoplasmic microtubules remained relatively short and tangled and exhibited a very distinct pattern as small stretches of microtubules. In addition, some microtubules formed around the nuclei, supporting the previous finding that the nuclear envelope can function as a microtubule-organizing center (19).

Nakiterpiosin does not alter centrosome organization

In principle, the inhibition of centrosomal microtubule regrowth could be caused by either defective nucleation or suppressed elongation. Nucleation at the centrosomes requires γ-tubulin and pericentrin (7), but nakiterpiosin did not affect the targeting of these two proteins to the centrosomes (Fig. 3C insets, and D left panels). Furthermore, EM analysis revealed that the centrosome in nakiterpiosin-treated cells maintained a normal organization, as shown by a pair of centrioles arranged perpendicularly to each other and made of 9 microtubule triplets surrounded by electron-dense matrix (Fig. 3D, right panel). We conclude that nakiterpiosin does not impair the centrosome structure or centrosome-mediated microtubule nucleation, but interferes with elongation of filaments.

Effects of nakiterpiosin on Golgi positioning and morphology

In addition to mitosis, microtubules are essential for interphase functions such as intracellular trafficking and organelle positioning. In particular, Golgi positioning in the perinuclear region is crucial for cell polarity and cell migration (20). Since nakiterpiosin influences the microtubule network, we examined whether the structure and function of the Golgi complex are affected. HeLa cells treated for 2 h with vehicle or the indicated agents were stained for the Golgi-resident protein GM130. In vehicle-treated cells, we observed the characteristic ribbon-like Golgi structure next to the nucleus (Fig. 4A, DMSO). Paclitaxel had little effect (Fig. 4A, PTX), but depolymerization of microtubules by nocodazole fragmented the Golgi into mini-stacks that were scattered throughout the cytoplasm (Fig. 4A, NOC). 5 μM nakiterpiosin, which interfered with spindle assembly, had no effect on Golgi morphology (Fig, 4A, NAK 5 μM). However, 25 μM nakiterpiosin, which impaired the organization of the centrosomal microtubule array, caused the Golgi ribbon to partially disperse, although the stacks were more interconnected compared to nocodazole treatment (Fig. 4A, NAK 25 μM). We further analyzed the Golgi structure by EM. Cells treated with vehicle or nakiterpiosin showed virtually indistinguishable Golgi stacks composed of closely apposed cisternae (Fig. 4B). Furthermore, we observed numerous budding profiles at the

rims of the cisternae (Fig. 4B), indicating that nakiterpiosin does not block vesicular transport.

Protein trafficking is not affected by nakiterpiosin

Next we tested whether nakiterpiosin influences protein transport through the Golgi to the plasma membrane. We microinjected a plasmid encoding the plasma membrane protein CD8 into HeLa cells, which do not express endogenous CD8. Cycloheximide was included during the microinjection period to prevent protein synthesis. We then removed the cycloheximide and incubated the cells with the indicated drugs for 90 min to allow expression and transport of CD8. The cells were then fixed without permeabilization and CD8 transported to the cell surface was detected using an antibody. As shown in Fig. 4C, CD8 was transported to the plasma membrane irrespective of the treatment (31-52 cells per condition). However, in nocodazole-treated cells, only about 1/3 of CD8 reached the cell surface, consistent with a previous report where nocodazole causes a delay in transport at early time points (data not shown; (21)). Therefore, although nakiterpiosin affects the overall organization of interphase microtubules at high concentration, it does not influence the transport of proteins to the cell surface, which may minimize the toxicity to interphase cells and enhance its specificity as an anti-mitotic drug.

Nakiterpiosin directly targets tubulin and suppresses microtubule polymerization in vitro

Since nakiterpiosin interferes with microtubule growth in cells, we tested whether it inhibits polymerization of highly purified tubulin *in vitro* (Fig. 5A). In DMSO tubulin polymerization was complete within 5 min, but was completely blocked by nocodazole as expected. In the presence of 1 μM nakiterpiosin, polymerization proceeded with an efficiency comparable to that of DMSO. In contrast, 5 μM and 10 μM nakiterpiosin strongly inhibited the reaction, and at 25 μM no polymerization was observed (Fig. 5A).

Next we examined the end products of the polymerization reactions by EM. At low magnification, long filaments were clearly visible in DMSO, 1 μM and 5 μM nakiterpiosin samples (Fig. 5B left panels, DMSO and NAK 5 μM). In addition, we also detected short polymers with few interspersed tubulin aggregates in the 5 μM sample (Fig. 5B left panels, NAK 5 μM). At 10 μM, more tubulin aggregates and short polymers were seen (data not shown). In samples treated with nocodazole or 25 μM nakiterpiosin, filaments were largely absent and, presumably due to fixation, large amounts of protein aggregates were observed instead (Fig. 5B left panels, NAK 25 μM and NOC). At high magnification, most filament ends displayed a straight conformation, which is an indication of growing microtubules (Fig. 5B right panels, DMSO). With increasing drug concentrations, shrinking microtubules became more abundant, as indicated by the banana-peel structure at the ends (Fig. 5B right panels, NAK 5 μM). Taken together, these data demonstrate that nakiterpiosin directly binds to tubulin and suppresses microtubule polymerization in a concentration-dependent manner.

Nakiterpiosin decreases microtubule polymer mass in cells

Since nakiterpiosin inhibits microtubule polymerization *in vitro*, we determined whether it influences polymer mass in cells. To evaluate the ratio of tubulin in polymers, HeLa cells were treated with vehicle or the indicated agents for 2 h and then lysed at room temperature in the presence of paclitaxel to stabilize all polymers. Polymer and soluble forms were separated and the amount of α-tubulin was analyzed by Western blotting. In vehicle-treated cells, about 2/3 of the tubulin was in polymers (8) (Fig. 5C, DMSO). Upon nocodazole treatment most of the tubulin became soluble (Fig. 5C, NOC), while paclitaxel treatment shifted the equilibrium towards polymers (Fig. 5C, PTX). Consistent with our immunofluorescence data, 5 μM nakiterpiosin did not change the polymer mass (Fig. 5C, 5 μM NAK). In contrast, 25 μM nakiterpiosin induced partial depolymerization and more than

half of the tubulin was present in the soluble form (Fig. 5C, 25 μM NAK). These results, together with our *in vitro* characterization, suggest that nakiterpiosin acts as a microtubule-depolymerizing agent both *in vitro* and in cells.

Nakiterpiosin enhances tubulin acetylation

Tubulin acetylation is thought to be an indication of microtubule stabilization and it occurs most efficiently after microtubule assembly (22, 23). To determine whether tubulin acetylation was affected by nakiterpiosin, the blots from the previous experiments were probed for acetylated α-tubulin. As expected, nocodazole depolymerized microtubules and abolished acetylation (Fig. 5D, NOC). In contrast, the microtubule-stabilizing agent paclitaxel increased tubulin acetylation by 7-fold (Fig. 5D, PTX). Surprisingly, while 5 μM nakiterpiosin had little effect on microtubule organization or cellular polymer mass (Figs. 3A and 5C, 5 μM NAK), tubulin acetylation was enhanced to a comparable extent as 1 μM paclitaxel treatment (Fig. 5D, 5 μM NAK). In addition, while 25 μM nakiterpiosin partially depolymerized microtubules in cells (Figs. 3A and 5C, 25 μM NAK), the acetylation of the remaining filaments was increased by 20-fold (Fig. 5D, 25 μM NAK). These data demonstrate that, unlike nocodazole which inhibits both tubulin polymerization and acetylation, nakiterpiosin inhibits the formation of new microtubules and simultaneously enhances the stability of existing filaments.

Nakiterpiosin inhibits the viability of paclitaxel-resistant cancer cells

Paclitaxel stabilizes microtubules, which blocks microtubule reorganization in early mitosis, thereby killing fast-proliferating cancer cells. Despite the routine use of paclitaxel in the treatment of ovarian, breast and lung cancers, tumor cells often have intrinsic or develop resistance to paclitaxel treatment. Since nakiterpiosin also stabilizes microtubules, we reason that nakiterpiosin might be effective to eliminate cancer cells that respond poorly to paclitaxel. We tested this possibility with NCI-H1155 and HCC366 cells, which are two human non-small-cell lung cancer cell lines (11) that show different degrees of paclitaxel resistance (Fig. 6A). After 48 h treatment with vehicle or varying concentrations of paclitaxel, we measured the cellular ATP level of HeLa and the two cancer cell lines to determine cell viability. 66% and 87% of NCI-H1155 and HCC366 cells were still viable after 48 h in 100 nM and 1 μM paclitaxel respectively, whereas most HeLa cells died under these two conditions (42% survival in 100 nM and 9% survival in 1 μM paclitaxel) (Fig. 6A). We then compared the viability of HeLa and NCI-H1155 cells treated with nakiterpiosin or 100 nM paclitaxel. Consistent with our results (Figs. 2A and 6A), HeLa cells were killed by both drugs (Fig. 6B). By contrast, although NCI-H1155 cells were refractory to paclitaxel, their proliferation was significantly reduced from 66% in 100 nM paclitaxel to 30% and 9% in 5 μM and 25 μM nakiterpiosin respectively(Fig. 6B). A similar inhibition was also observed in HCC366 cells treated with nakiterpiosin, which decreased cell viability from 86% in 1 μM paclitaxel to 60% and 39% in 5 μM and 25 μM nakiterpiosin respectively (Fig. 6C). These data imply that nakiterpiosin acts through a different mechanism than paclitaxel. In conclusion, our results demonstrate the effectiveness of nakiterpiosin in killing cancer cells as well as the potential to be applicable to a broad spectrum of tumors.

Discussion

Microtubule-targeting drugs have been used with remarkable success in cancer chemotherapy. However, despite their extensive use in treating various types of cancers, several problems remain unsolved (24). In particular, patients often develop drug resistance due to repeated exposure to the same chemical agent. Differential expression of multiple tubulin isotypes may also compromise drug efficiency in certain tissues (25). To overcome

these limitations, tremendous efforts have been made to develop agents that either bind to or act differently on microtubules. In addition, combination therapy with two or more anti-microtubule drugs improves drug efficiency as well as minimizes toxicity (24). Thus, new microtubule-targeting compounds can significantly impact cancer treatment. In the current study, we identify nakiterpiosin as a novel anti-mitotic agent that suppresses microtubule dynamics and triggers cell death in cancer cells (Figs. 2A, 6B, and 6C).

Nakiterpiosin was originally extracted from a marine sponge that grows on corals and causes the destruction of large areas of coral reefs (9). It was shown to have potent cytotoxicity against mouse leukemia cells (9), but the cellular target and mechanism of action were unknown. Our results demonstrate that nakiterpiosin targets microtubules and induces cell death by interfering with mitotic progression. At or below 1 μM, nakiterpiosin has little or no effect on cell division when observed by time-lapse microscopy (Fig. 2A) and only marginal effects on cell cycle progression when analyzed by FACS (10). However, cells that enter mitosis in the presence of 5 μM or greater concentrations of nakiterpiosin form aberrant spindles (Fig. 2C) and become arrested (Fig. 2A) due to activation of the spindle assembly checkpoint (Fig. 2B). Upon prolonged arrest, cells undergo mitotic catastrophe, a form of cell death that occurs during mitosis (16). The mitotic inhibition is fully reversible and arrested cells divide upon drug removal (Fig. 2A), suggesting that nakiterpiosin does not permanently damage cells. Protein secretion and viability of interphase cells are also not impaired at this concentration (Fig. 3C). Altogether, our results show that nakiterpiosin induces mitotic cell death by perturbing spindle dynamics with little effect on interphase cells.

In vitro microtubule polymerization from purified tubulin is completely abolished by a high concentration of nakiterpiosin (Fig. 5A), demonstrating that nakiterpiosin directly binds to tubulin. This is consistent with the finding that, in interphase cells treated at the same concentration, the amount of tubulin incorporated into polymers is markedly reduced (Fig. 5C). Moreover, the organization of the microtubule network is altered under this condition (Fig. 3A). Unlike nocodazole-treated cells where the microtubules are completely depolymerized, filaments are still present in nakiterpiosin-treated cells, although the microtubules appear to be tangled and shorter. Strikingly, these filaments no longer originate from the centrosomes.

In addition to reducing cellular polymer mass, nakiterpiosin negatively regulates microtubule dynamics, as shown by the loss of EB1 from the microtubule tips (Fig. 3B). EB1 is a microtubule plus end-tracking protein that preferentially binds to the tip of growing filaments (26). Reduced EB1 end labeling suggests that microtubules become less dynamic. Another line of evidence that nakiterpiosin perturbs microtubule dynamics comes from the dramatic increase in tubulin acetylation (Fig. 5D). Tubulin acetylation is thought to be an indication of microtubule stabilization and it occurs most efficiently after microtubule assembly (22, 23). In contrast to nocodazole treatment, microtubules are still present and become highly acetylated in nakiterpiosin-treated cells (Figs. 3A, 5C, and 5D), despite the fact that it interferes with microtubule polymerization *in vitro* and in cells (Fig. 5A-C). Thus, the increase in tubulin acetylation in nakiterpiosin-treated cells is presumably an outcome of suppressed microtubule dynamics. In the regrowth assay, nakiterpiosin strongly inhibits polymerization of new filaments from the centrosomes (Fig. 3C), but the centrosomes appear unaltered when analyzed by EM and immunofluorescence (Fig. 3D). In addition, although the Golgi could function as a nucleation site for microtubules (27, 28), filament formation is suppressed in the perinuclear area where the Golgi is localized (Fig. 3C). These findings, together with enhanced tubulin acetylation, suggest that nakiterpiosin simultaneously stabilizes existing filaments and prevents formation of new microtubules.

In addition to the unique properties described above, nakiterpiosin has a very different chemical structure and mechanism of action compared to other microtubule-targeting drugs such as paclitaxel (Figs. 1 and 6) (10). Paclitaxel perturbs mitotic progression by stabilizing microtubules, which increases tubulin acetylation (Fig. 5D) (23). Several studies have provided evidence that tubulin acetylation is linked to drug resistance (23, 29, 30). In particular, acquisition of paclitaxel resistance in tumors is one of the most challenging obstacles to successful cancer chemotherapy. Cancer cells can develop paclitaxel resistance by acquiring mutations in β-tubulin (31). Intriguingly, paclitaxel-resistant cells have reduced levels of acetylated tubulin and less stable filaments (31). Since nakiterpiosin stimulates tubulin acetylation more effectively than paclitaxel and interferes with microtubule dynamics differently, it could be used as a chemotherapeutic agent against paclitaxel-resistant tumors. Indeed, our data show that nakiterpiosin reduces the viability of two paclitaxel-resistant cancer cell lines (Fig. 6). Furthermore, nakiterpiosin could be used in combination with other microtubule-targeting drugs to improve efficiency or minimize toxicity. In summary, here we report the cellular target and biological effects of nakiterpiosin and suggest its potential use in cancer chemotherapy.

Supplementary Material

Refer to Web version on PubMed Central for supplementary material.

Acknowledgments

We thank Chuo Chen for the generous gift of nakiterpiosin, Christopher Gilpin and Tom Januszewski for EM assistance, Michael White for NCI-H1155 and HCC366 cell lines, Martin Lowe and Keith Gull for antibodies, Dorothy Mundy, Chih-Wen Chu and Katie Zhang for critical reading of the manuscript. J.S. is a Virginia Murchison Lithicum Scholar in Medical Research and supported by grants from the American Heart Association (8065090F) and the NIH (GM096070).

References

1. Gascoigne KE, Taylor SS. How do anti-mitotic drugs kill cancer cells? J Cell Sci. 2009; 122:2579–85. [PubMed: 19625502]
2. Walczak CE, Heald R. Mechanisms of mitotic spindle assembly and function. Int Rev Cytol. 2008; 265:111–58. [PubMed: 18275887]
3. Bornens M. Organelle positioning and cell polarity. Nat Rev Mol Cell Biol. 2008; 9:874–86. [PubMed: 18946476]
4. Lane J, Allan V. Microtubule-based membrane movement. Biochim Biophys Acta. 1998; 1376:27–55. [PubMed: 9666066]
5. Berbari NF, O'Connor AK, Haycraft CJ, Yoder BK. The primary cilium as a complex signaling center. Curr Biol. 2009; 19:R526–35. [PubMed: 19602418]
6. Mitchison T, Kirschner M. Dynamic instability of microtubule growth. Nature. 1984; 312:237–42. [PubMed: 6504138]
7. Luders J, Stearns T. Microtubule-organizing centres: a re-evaluation. Nat Rev Mol Cell Biol. 2007; 8:161–7. [PubMed: 17245416]
8. Zhai Y, Kronebusch PJ, Simon PM, Borisy GG. Microtubule dynamics at the G2/M transition: abrupt breakdown of cytoplasmic microtubules at nuclear envelope breakdown and implications for spindle morphogenesis. J Cell Biol. 1996; 135:201–14. [PubMed: 8858174]
9. Teruya T, Nakagawa S, Koyama T, Arimoto H, Kita M, Uemura D. Nakiterpiosin and nakiterpiosinone, novel cytotoxic C-nor-D-homosteroids from the Okinawan sponge Terpios hoshinota. Tetrahedron. 2004; 60:6989–93.
10. Gao S, Wang Q, Huang LJ, Lum L, Chen C. Chemical and biological studies of nakiterpiosin and nakiterpiosinone. J Am Chem Soc. 2010; 132:371–83. [PubMed: 20000429]

11. Whitehurst AW, Bodemann BO, Cardenas J, et al. Synthetic lethal screen identification of chemosensitizer loci in cancer cells. Nature. 2007; 446:815–9. [PubMed: 17429401]
12. Wei JH, Seemann J. The mitotic spindle mediates inheritance of the Golgi ribbon structure. J Cell Biol. 2009; 184:391–7. [PubMed: 19188490]
13. Wang Y, Wei JH, Bisel B, Tang D, Seemann J. Golgi Cisternal Unstacking Stimulates COPI Vesicle Budding and Protein Transport. PLoS ONE. 2008; 3:e1647. [PubMed: 18297130]
14. Wei JH, Seemann J. Induction of asymmetrical cell division to analyze spindle-dependent organelle partitioning using correlative microscopy techniques. Nat Protoc. 2009; 4:1653–62. [PubMed: 19876022]
15. Sandoval IV, Weber K. Different tubulin polymers are produced by microtubule-associated proteins MAP2 and tau in the presence of guanosine 5'-(alpha, beta-methylene)triphosphate. J Biol Chem. 1980; 255:8952–4. [PubMed: 6773956]
16. Castedo M, Perfettini JL, Roumier T, Andreau K, Medema R, Kroemer G. Cell death by mitotic catastrophe: a molecular definition. Oncogene. 2004; 23:2825–37. [PubMed: 15077146]
17. Jordan MA, Wilson L. Microtubules as a target for anticancer drugs. Nat Rev Cancer. 2004; 4:253–65. [PubMed: 15057285]
18. Lansbergen G, Akhmanova A. Microtubule plus end: a hub of cellular activities. Traffic. 2006; 7:499–507. [PubMed: 16643273]
19. Tassin AM, Maro B, Bornens M. Fate of microtubule-organizing centers during myogenesis in vitro. J Cell Biol. 1985; 100:35–46. [PubMed: 3880758]
20. Bisel B, Wang Y, Wei JH, et al. ERK regulates Golgi and centrosome orientation towards the leading edge through GRASP65. J Cell Biol. 2008; 182:837–43. [PubMed: 18762583]
21. Cole NB, Sciaky N, Marotta A, Song J, Lippincott-Schwartz J. Golgi dispersal during microtubule disruption: regeneration of Golgi stacks at peripheral endoplasmic reticulum exit sites. Mol Biol Cell. 1996; 7:631–50. [PubMed: 8730104]
22. Matsuyama A, Shimazu T, Sumida Y, et al. In vivo destabilization of dynamic microtubules by HDAC6-mediated deacetylation. The EMBO journal. 2002; 21:6820–31. [PubMed: 12486003]
23. Piperno G, LeDizet M, Chang XJ. Microtubules containing acetylated alpha-tubulin in mammalian cells in culture. J Cell Biol. 1987; 104:289–302. [PubMed: 2879846]
24. Kavallaris M. Microtubules and resistance to tubulin-binding agents. Nat Rev Cancer. 2010; 10:194–204. [PubMed: 20147901]
25. Luduena RF. Multiple forms of tubulin: different gene products and covalent modifications. Int Rev Cytol. 1998; 178:207–75. [PubMed: 9348671]
26. Komarova Y, De Groot CO, Grigoriev I, et al. Mammalian end binding proteins control persistent microtubule growth. J Cell Biol. 2009; 184:691–706. [PubMed: 19255245]
27. Rivero S, Cardenas J, Bornens M, Rios RM. Microtubule nucleation at the cis-side of the Golgi apparatus requires AKAP450 and GM130. The EMBO journal. 2009; 28:1016–28. [PubMed: 19242490]
28. Efimov A, Kharitonov A, Efimova N, et al. Asymmetric CLASP-dependent nucleation of noncentrosomal microtubules at the trans-Golgi network. Dev Cell. 2007; 12:917–30. [PubMed: 17543864]
29. Sangrajrang S, Denoulet P, Laing NM, et al. Association of estramustine resistance in human prostatic carcinoma cells with modified patterns of tubulin expression. Biochem Pharmacol. 1998; 55:325–31. [PubMed: 9484799]
30. Geyp M, Ireland CM, Pittman SM. Increased tubulin acetylation accompanies reversion to stable ploidy in vincristine-resistant CCRF-CEM cells. Cancer Genet Cytogenet. 1996; 87:116–22. [PubMed: 8625256]
31. Hari M, Loganzo F, Annable T, et al. Paclitaxel-resistant cells have a mutation in the paclitaxel-binding region of beta-tubulin (Asp26Glu) and less stable microtubules. Mol Cancer Ther. 2006; 5:270–8. [PubMed: 16505100]

Abbreviations

DMSO	dimethyl sulfoxide
EM	electron microscopy
Hh	Hedgehog
NAK	nakiterpiosin
NOC	nocodazole
PTX	paclitaxel
SAC	spindle assembly checkpoint

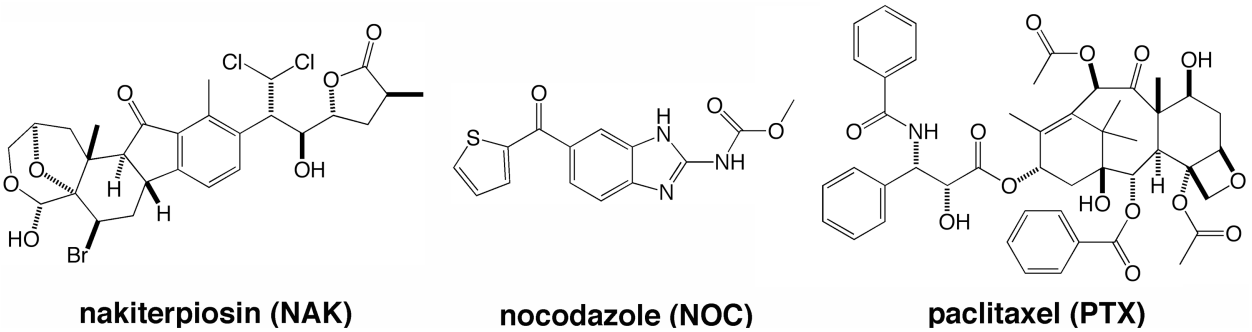

Figure 1.
Chemical structures of nakiterpiosin (NAK), nocodazole (NOC) and paclitaxel (PTX).

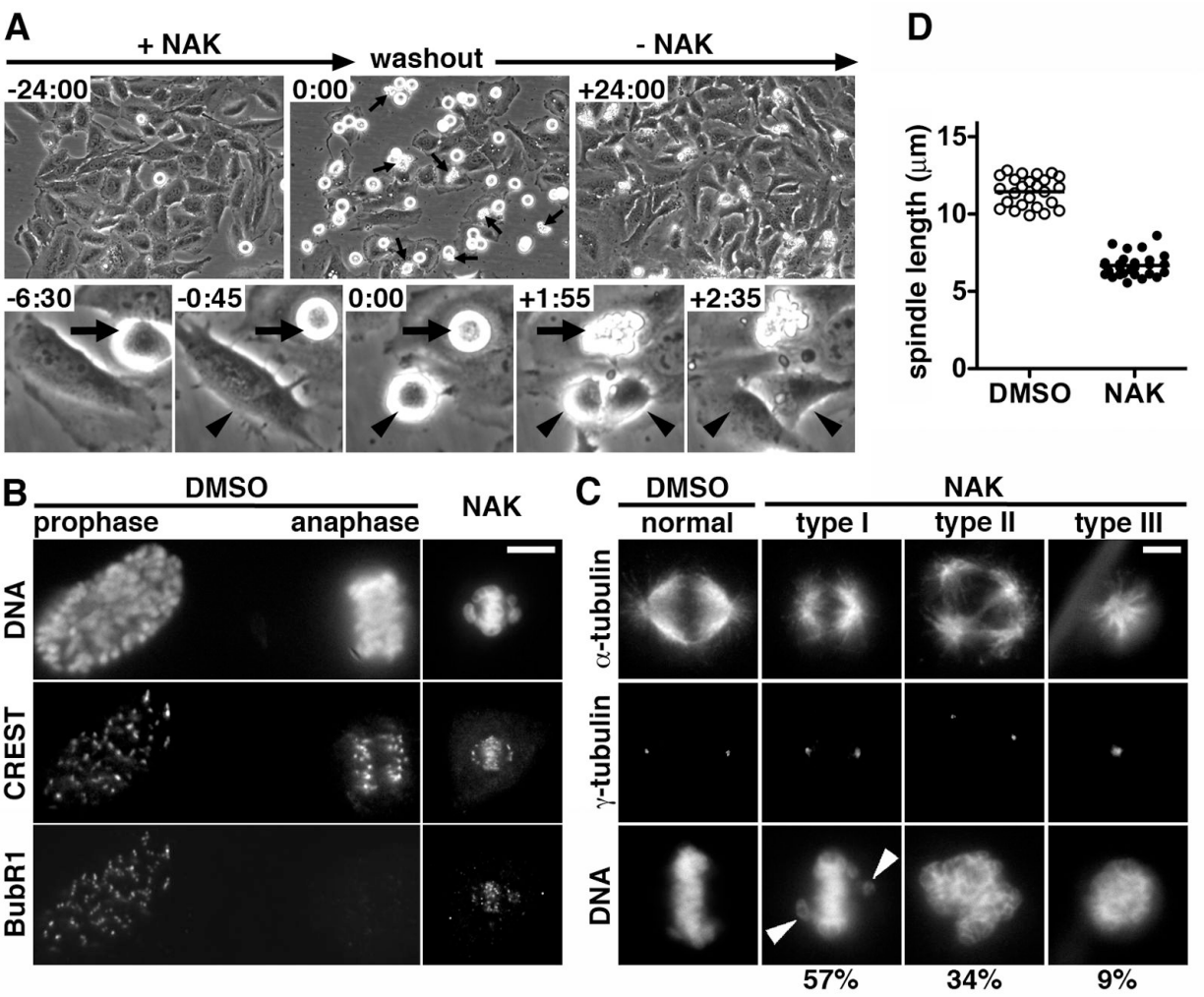

Figure 2. Nakiterpiosin arrests cells in mitosis and causes mitotic catastrophe by impairing spindle assembly

A, Nakiterpiosin causes mitotic arrest and cell death. Still images at the time points indicated in hh:mm from a representative phase-contrast time-lapse movie ($n = 3$). HeLa cells were imaged for 24 h in 10 μM NAK (-24:00). The drug was washed out (0:00) and the cells were imaged in fresh medium without the drug for another 24 h (+24:00). Arrows indicate cells undergoing mitotic catastrophe (mitotic cell death). The lower panels show two representative cells at higher magnification. Arrowheads indicate a NAK-treated cell that entered mitosis (-0:45), became arrested (0:00) and divided (+1:55) after washout. Arrows point to a cell that underwent prolonged mitotic arrest (-6:30) and subsequent cell death (+1:55).

B-D, HeLa cells were treated for 2 h with DMSO or 5 μM NAK and labeled for DNA, BubR1 and with CREST serum to mark kinetochores (B) or for α-tubulin, γ-tubulin and DNA (C and D).

B, The spindle assembly checkpoint is activated in NAK-treated cells, as indicated by BubR1 recruitment to kinetochores. Vehicle-treated cells in prophase and anaphase were located next to each other in the same field. Bar, 10 μm.

C, Nakiterpiosin arrests cells in mitosis with aberrant spindles. 57% of the NAK-arrested cells assembled bipolar-like spindles with uncongressed chromosomes (type I), 34% formed

multiple asters (type II) and 9% developed monopolar spindles (type III) (170 mitotic cells counted). Bar, 5μm.

D, The spindle length was measured as the distance between two γ-tubulin foci at metaphase spindle poles. The interpolar distance was significantly decreased by 42%, from 11.5 ± 0.2 μm in DMSO-treated cells to 6.7 ± 0.1 μm in NAK-treated cells (mean ± SEM; 25-27 spindles per condition; $P < 0.0001$).

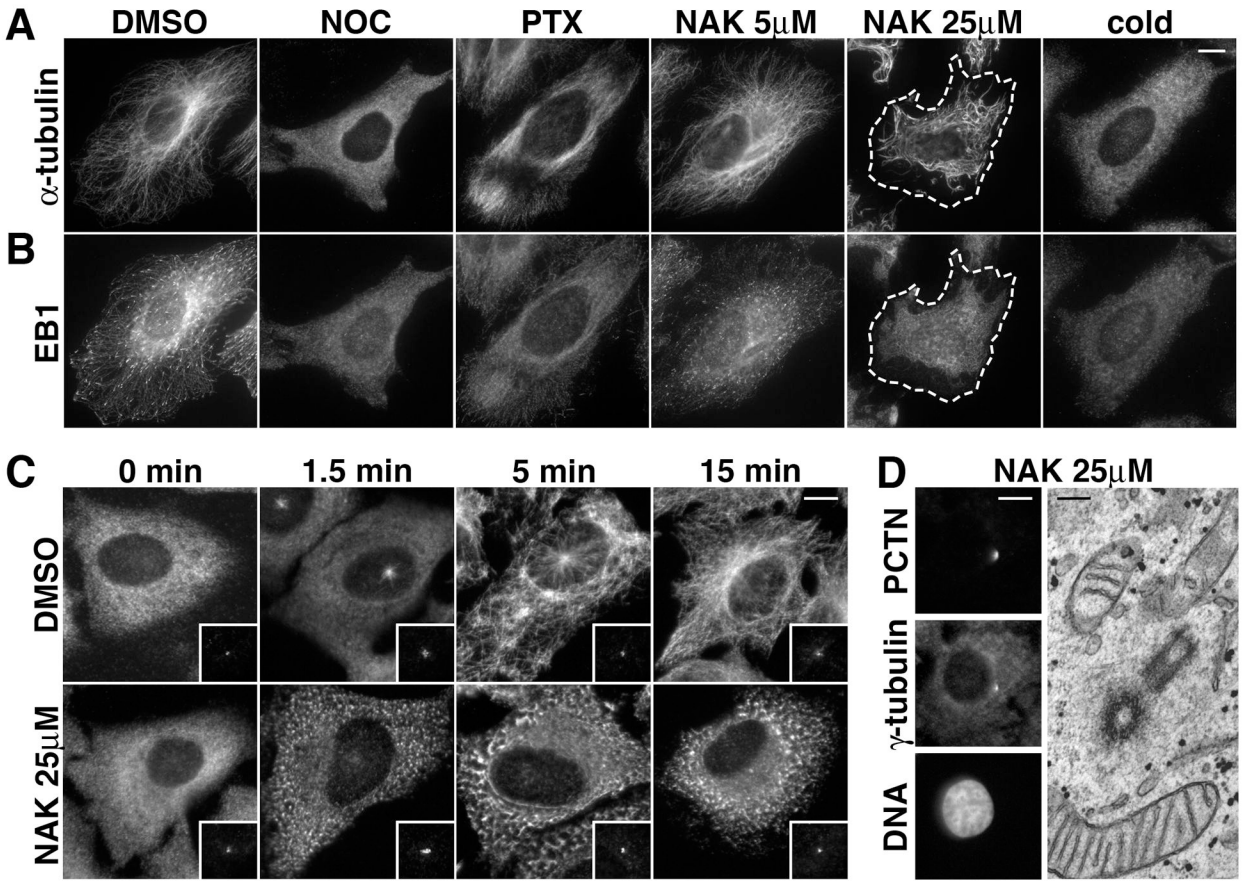

Figure 3. Nakiterpiosin suppresses microtubule dynamics in interphase cells

A and B, HeLa cells were treated for 2 h with DMSO, 5 μg/ml nocodazole (NOC), 1 μM paclitaxel (PTX), 5 or 25 μM nakiterpiosin (NAK), or cooled on ice for 30 min (cold). The cells were then fixed and labeled for α-tubulin (A) and EB1 (B). Bar, 10 μm.

A, In 25 μM NAK microtubules no longer originated from the centrosomes and became shorter (The cell border is outlined with dash lines). 5 μM NAK and DMSO showed little or no effect. B, EB1 was concentrated at the tips of microtubules in DMSO but not in 25 μM NAK, suggesting NAK suppresses microtubule dynamics.

C, Centrosome-mediated microtubule regrowth is inhibited by 25 μM NAK. HeLa cells were cooled on ice for 30 min to depolymerize microtubules and incubated on ice for 30 min with DMSO or 25 μM NAK (0 min). The cells were then warmed to 37°C, fixed at the indicated time points and double-labeled for α-tubulin and pericentrin (insets). Bar, 10 μm.

D, Nakiterpiosin does not alter centrosome organization. HeLa cells treated for 2 h with 25 μM NAK were either immunolabeled for pericentrin (PCTN), γ-tubulin and DNA (left panels, bar, 10μm) or analyzed by EM (right panel, bar, 200 nm).

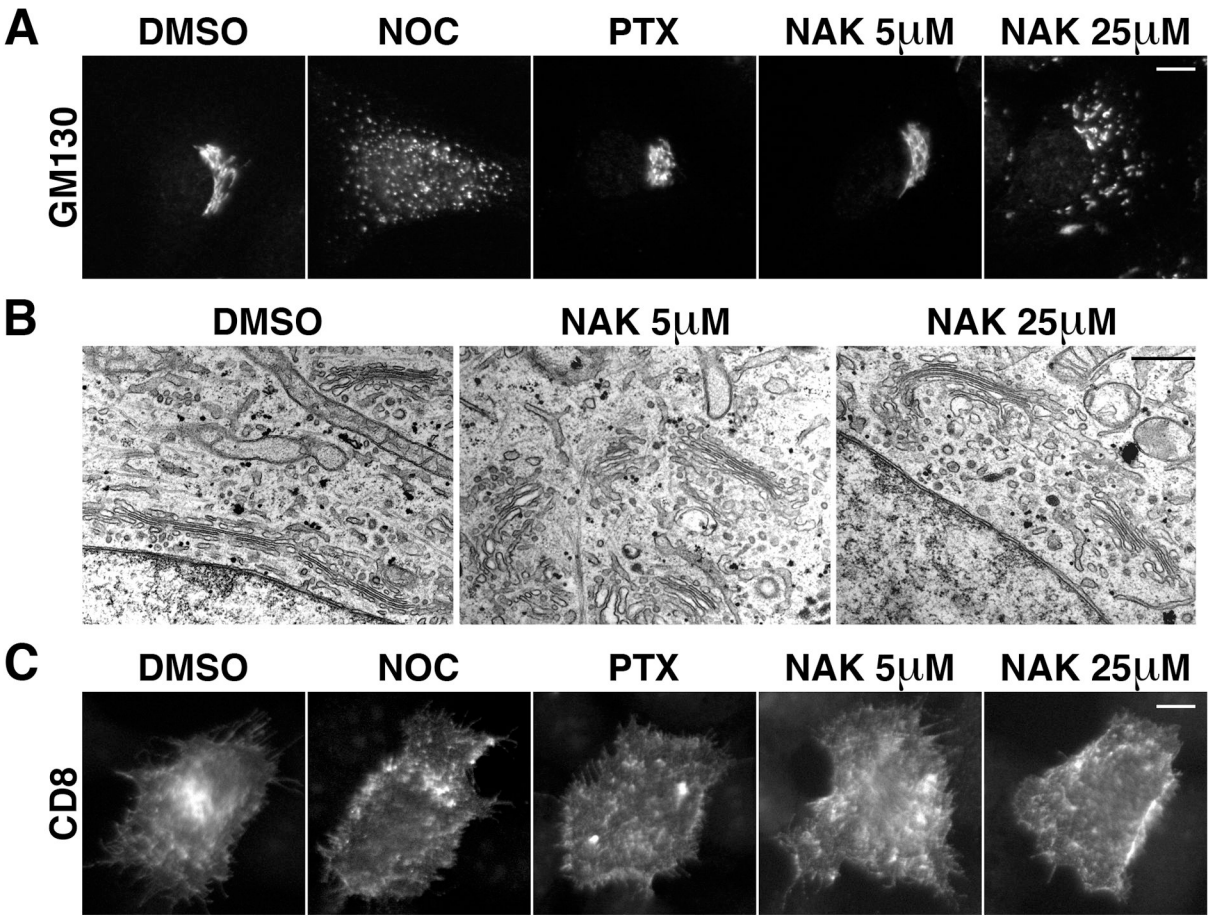

Figure 4. Effects of nakiterpiosin on Golgi morphology and protein transport

HeLa cells treated for 2 h with DMSO or the indicated drugs were either immunolabeled for the Golgi-resident protein GM130 (A) or analyzed by EM (B).

A, The Golgi ribbon is partially dispersed by 25 μM NAK but not by 5 μM NAK. Bar, 10 μm.

B, The structure of Golgi stacks composed of closely apposed cisternae is not altered by NAK. Bar, 500 nm.

C, CD8 transport through the secretory pathway is not affected by NAK. A plasmid encoding the plasma membrane protein CD8 was microinjected into HeLa cells in the presence of cycloheximide. The cells were released from the cycloheximide block, incubated for 90 min with the indicated agents at 37°C, fixed and immunolabeled for CD8 at the cell surface without permeabilization. Bar, 10 μm.

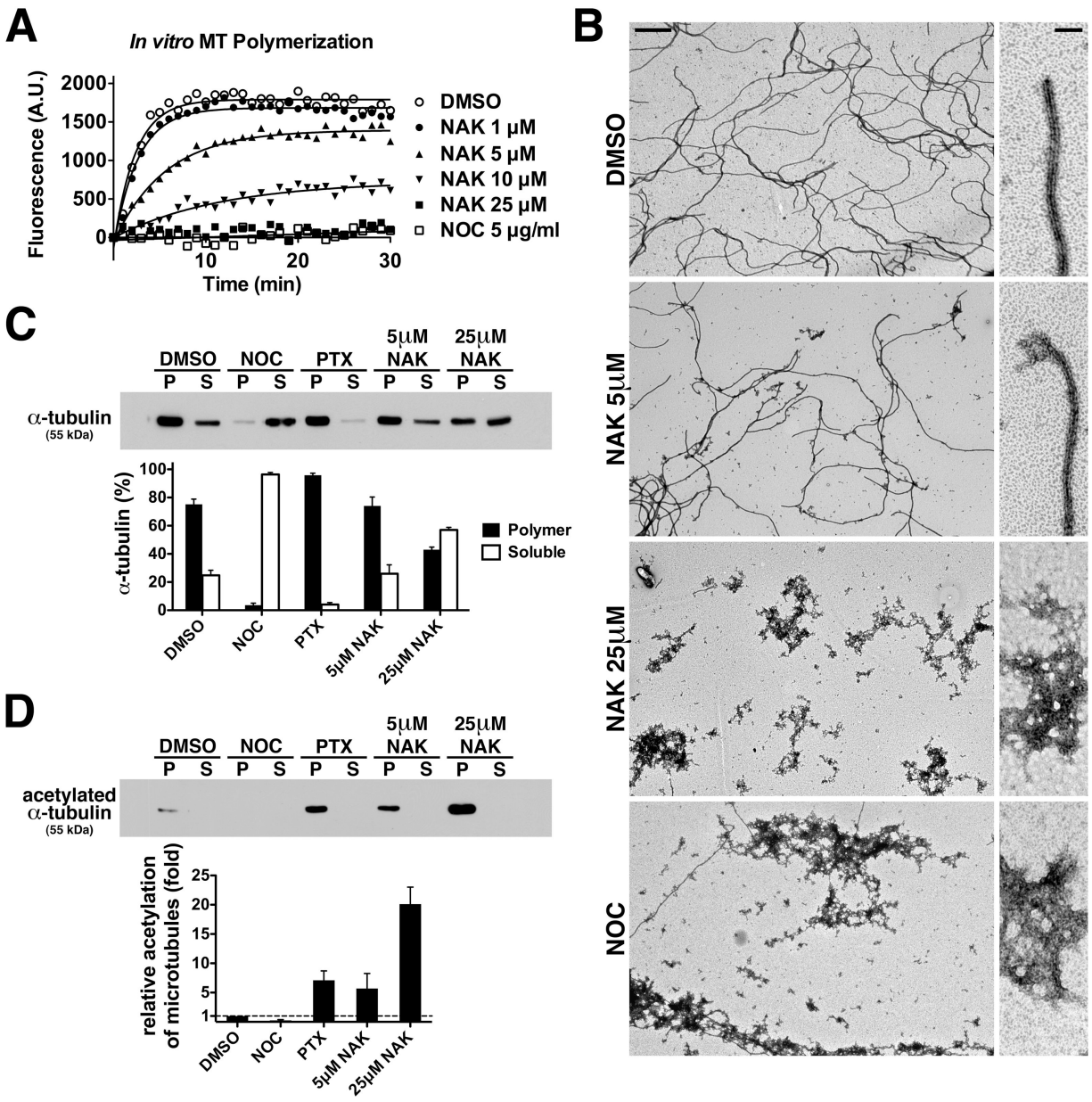

Figure 5. Nakiterpiosin inhibits microtubule polymerization *in vitro* and in cells and enhances tubulin acetylation

A, Nakiterpiosin inhibits microtubule polymerization *in vitro* in a concentration-dependent manner. Microtubule polymerization from purified tubulin at 37°C with vehicle or the indicated drugs was monitored by an increase in fluorescence.

B, The end products of the polymerization reactions were fixed, negatively stained and analyzed by EM. At low magnification (left panels, bar, 1 μm), filamentous polymers were observed in 5 μM NAK, although they appeared shorter than in DMSO. No polymers but tubulin aggregates were detected in 25 μM NAK and NOC. At higher magnification (right panels, bar, 100 nm), most filament ends were straight, indicating growing microtubules (DMSO). As NAK concentration increased, microtubule ends frequently showed banana-peel structures, indicating shrinking microtubules (5 μM).

C and D, HeLa cells treated for 2 h with vehicle or the indicated agents were lysed at room temperature. Tubulin in polymers was separated from soluble tubulin by centrifugation. Equal fractions of the supernatant (S) and the pellet (P) were analyzed by Western blotting for α-tubulin or acetylated α-tubulin and band intensity was quantified ($n = 3$).
C, The microtubule polymer mass in cells is decreased by 25 μM NAK.
D, Nakiterpiosin enhances tubulin acetylation.

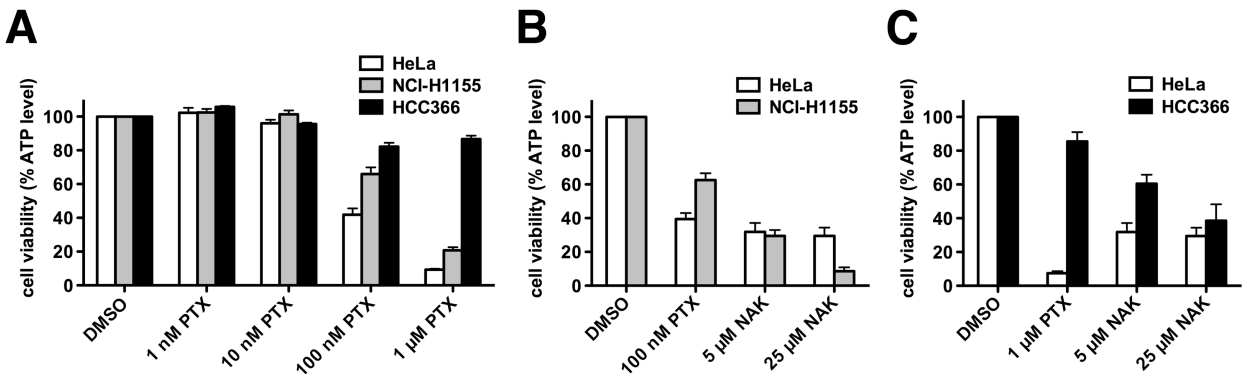

Figure 6. Nakiterpiosin reduces the viability of paclitaxel-resistant cancer cells

HeLa, NCI-H1155 and HCC366 cells were treated for 48 h with DMSO or the indicated drugs. Cell viability was then determined by the relative amount of ATP present (normalized to DMSO-treated cells) using the CellTiter-Glo assay.

A. NCI-H1155 and HCC366 cells show different levels of paclitaxel resistance ($n = 3$).

B, Nakiterpiosin reduces cell viability of NCI-H1155 cells ($n = 4$).

C, Nakiterpiosin reduces cell viability of HCC366 cells ($n = 5$).